

Theory of Home Range Estimation from Mark-Recapture Measurements of Animal Populations

L. Giuggioli ^a, G. Abramson ^{a,b}, V. M. Kenkre ^a

^a*Consortium of the Americas for Interdisciplinary Science and Department of Physics, University of New Mexico, Albuquerque, NM 87131, USA.*

^b*Centro Atómico Bariloche, CONICET and Instituto Balseiro, 8400 San Carlos de Bariloche, Río Negro, Argentina.*

R. R. Parmenter, T. L. Yates

Department of Biology, University of New Mexico, Albuquerque, NM 87131, USA.

Abstract

A theory is provided for the estimation of home ranges of animals from the standard mark-recapture technique in which data are collected by capturing, tagging and recapturing the animals. The theoretical tool used is the Fokker-Planck equation, its characteristic quantities being the diffusion constant which describes the motion of the animals, and the attractive potential which addresses their tendency to live near their burrows. The measurement technique is shown to correspond to the calculation of a certain kind of mean square displacement of the animals relevant to the specific probing window in space corresponding to the trapping region. The output of the theory is a sigmoid curve of the observable mean square displacement as a function of the ratio of distances characteristic of the home range and the trapping region, along with an explicit prescription to extract the home range from observations. Applications of the theory to rodent movement in Panama and New Mexico are pointed out. An analysis is given of the sensitivity of our theory to the choice of the confining potential via the use of various representative cases. A comparison is provided between home range size inferred from our method and from other procedures employed in the literature. Consequences of home range overlap are also discussed.

Key words: Animal diffusion, Home range size, Home range overlap

Email addresses: giuggiol@unm.edu (L. Giuggioli),
abramson@cab.cnea.gov.ar (G. Abramson), kenkre@unm.edu (V. M. Kenkre),
bparmenter@vallescaldera.gov (R. R. Parmenter), tyates@unm.edu (T. L. Yates).

1 Introduction

The use of space by animals is the result of a combination of internal factors, such as the physiology and morphology of the animal, and external factors such as the environment. It is well known that mammals, in order to conduct their daily activity, occupy only part of their available environment: the so-called home range (Burt, 1943). A recent study on the scaling of home range size as function of animal body mass or metabolic rate (Jetz et al., 2004) shows that the home range dimensions are a compromise between two ingredients: the necessity for harvesting resources and the detection and response to intrusion. On one hand, the home range has to be large enough to meet energy requirements; on the other, it has to be small enough for the resident to be protected from intrusions of same-species foraging neighbours (Buskirk, 2004). The importance of learning about home ranges stems not only from the intellectual need to understand animal movement (Okubo, 1979), but also from the practical value in the determination of the size of the home range: it is intimately related to a variety of ecological phenomena ranging from social organization to mating behavior and disease transmission (Wolff, 1997; Yates et al., 2002; Parmenter and MacMahon, 1983; Abramson and Kenkre, 2002; Abramson et al., 2003; Kenkre, 2003, 2004; Kenkre et al., 2004). There is already a body of biological literature on home ranges and related animal movements (Okubo, 1979; Murray, 1993). It is useful to build upon that literature to provide a comprehensive mathematical description of the dynamics of ecological systems.

Given the spatial probability distribution for an individual, the home range size has been typically defined as the contour that contains a fixed percentage (usually 95%) of the total volume under the distribution (Jennrich and Turner, 1969; Ford and Krumme, 1979). Home range size can be estimated from data of recorded locations over a sufficiently large period of time. These data can be obtained through a variety of methods including radio tracking and live trapping. Different techniques have been proposed for estimating home range size from location data of *single* animals (see e.g. the review by Worton (1987)). The various approaches can be divided into three categories. In the first, estimates are made using the peripheral points of the location data. In the second, the data are fitted to a pre-assumed probability distribution. In the third, the probability distribution is determined only from the statistical properties of the data (such as the one proposed by Anderson (1982)). The first method gives the maximum extent of the animal's range while the other two methods give a profile of the probability distribution inside the home range.

In order to obtain reasonable accuracy, all three procedures have the requirement that the number of locations recorded for each animal be large (Ford and Krumme, 1979). Unless unusual efforts are made during the field sampling, the number

of locations for each individual is typically not very large (e.g. Mares et al. (1980); Bergstrom (1988)). On the other hand, the number of individuals is typically quite large. Home range estimation from location data of *many* individuals, therefore, avoids such problems (Ford and Krumme, 1979): the positions are averaged over all the animals recorded.

The purpose of the present paper is to develop a theoretical model which gives a simple prescription for the extraction of home range parameters from location data of animal population inside a limited region of space. Such a limited window of observation represents, for example, the size of the trapping array in a mark-recapture experiment, in which an animal is captured, tagged and then recorded every time it is recaptured (Parmenter et al., 2003).

In the model we suggest, the motion of each animal is represented by diffusion in a confining potential, the latter representing the attraction of the animal to the home-place, the burrow. The potential has a characteristic width associated with the size of the home range, which we call L . The underlying equation in our approach is the Fokker-Planck equation for the probability distribution for each individual (Okubo, 1979; Risken, 1989). The stationary solution of this Fokker-Planck equation is used to calculate the infinite-time limit of the mean square displacement saturation value of all the individuals as function of L . Comparison with the measured mean square displacement allows then the determination of the home range size, expressed here in units of length. The home range size has been typically denoted in the literature in term of an area. The relation to our description is simply that that area is given by the product of L for the two directions. Application of our procedure to rodent measurements in Panama and in New Mexico may be found in (Giuggioli et al., 2004; Abramson et al., 2004) where our model in its simplest form has been successfully used to extract not only home range sizes but also diffusion constants from mark-recaptures of rodent populations.

The practical output of our present theoretical procedure is a saturation curve for the observed mean square displacement as a function of L/G , the ratio of the home range to G , a length that is characteristic of the size of the observation window. We predict a sigmoid shape for the saturation curve. An immediate consequence is that, for the greatest accuracy in the measurement of the home range, the observation window should be of the order of the home range. For certain potentials it is possible to write down simple analytical expressions for the saturation curve. For others the curve is obtained through numerical computation. Our theory also addresses the distribution of home ranges according to habitat, equivalently home range overlap, a quantity independently accessible through allometric scaling arguments (Jetz et al., 2004).

The paper is organized as follows. The general problem of calculating the average mean square displacement for a population of individuals, each one living

in its own home range, and observed only inside a spatially limited window, is addressed in Sec. 2. The sensitivity of the saturation curve to the choice of the confining potential is studied in Sec. 3 through various representative cases. The case of a non-uniform distribution of home ranges and considerations for experimentally determining the average inter-home distance (related to the home range overlap) is the subject of Sec. 4. The comparison between home range size inferred from our method and the so-called convex polygon method, usually employed in the literature, forms Sec. 5, and conclusions are in Sec. 6.

2 Mean square displacement in a probing window: general considerations

We model the motion of an animal living in its home range through the Fokker-Planck equation for the probability distribution $\mathcal{P}(x, t)$

$$\frac{\partial \mathcal{P}(x, t)}{\partial t} = \frac{\partial}{\partial x} \left[\frac{dU(x)}{dx} \mathcal{P}(x, t) \right] + D \frac{\partial^2 \mathcal{P}(x, t)}{\partial x^2}, \quad (1)$$

wherein D is the diffusion coefficient of the animal and $U(x)$ is the potential in which the animal is forced to roam. The potential $U(x)$ is a representation of the bias or reduced randomness associated with the walk. A pure random walk as in a simple diffusive process has $U(x) = 0$. When $U(x) \neq 0$ we identify its characteristic length with the home range size L .

The 2-dimensional counterpart of Eq. (1), written in polar coordinates, is

$$\begin{aligned} \frac{\partial \mathcal{P}(r, \phi, t)}{\partial t} = & \frac{1}{r} \frac{\partial}{\partial r} \left[r \left(\frac{\partial U(r, \phi)}{\partial r} \mathcal{P}(r, \phi, t) + D \frac{\partial \mathcal{P}(r, \phi, t)}{\partial r} \right) \right] + \\ & \frac{1}{r^2} \frac{\partial}{\partial r} \left[\frac{\partial U(r, \phi)}{\partial \phi} \mathcal{P}(r, \phi, t) + D \frac{\partial \mathcal{P}(r, \phi, t)}{\partial \phi} \right]. \end{aligned} \quad (2)$$

The description provided by (2) would be appropriate for a wide range of animal motion contexts. The third dimension is very rarely required but can be easily incorporated. All the essential concepts are, however, easily represented through the description provided by the 1-dimensional version. Therefore, we restrict ourselves in the present paper to Eq. (1). It is straightforward to generalize all considerations to higher dimensions if required.

The overall characteristics of the motion can be obtained by calculating just the moments of the distribution $\mathcal{P}(x, t)$ rather than the full $\mathcal{P}(x, t)$ which entails an integration of the probability. In a typical experiment a probing window is used, i.e., the animal is observed only inside a limited region of

space, as in a trapping array in a mark-recapture experiment. The integration to calculate the moments is then performed only over the probing window. The second moment of $\mathcal{P}(x, t)$, i.e., the mean square displacement, is given by

$$\langle \Delta x^2(t) \rangle = \frac{\int_{-G/2}^{G/2} dx (x - x_0)^2 \mathcal{P}_{x_0}(x, t)}{\int_{-G/2}^{G/2} dx \mathcal{P}_{x_0}(x, t)}, \quad (3)$$

where G is the dimension of the window and x_0 is the position of the animal at time $t = 0$. Because initially each animal can be anywhere inside G , the numerator and denominator of Eq. (3) have to be averaged over all the possible initial positions inside the window. We then have, for the average,

$$\langle \langle \Delta x^2(t) \rangle \rangle = \frac{\int_{-G/2}^{G/2} dx_0 \int_{-G/2}^{G/2} dx (x - x_0)^2 \mathcal{P}_{x_c, x_0}(x, 0) \mathcal{P}_{x_c, x_0}(x, t)}{\int_{-G/2}^{G/2} dx_0 \int_{-G/2}^{G/2} dx \mathcal{P}_{x_c, x_0}(x, 0) \mathcal{P}_{x_c, x_0}(x, t)}. \quad (4)$$

We have introduced here the label x_c to represent the burrow position of each animal. Equation (4) is the contribution to the mean square displacement of an animal whose burrow is at x_c . A further average over the distribution of burrow positions is necessary. If this distribution is denoted by $\rho(x_c)$, the observed mean square displacement within the window of size G is given by

$$\overline{\Delta x^2(t)} = \frac{\int_{-\infty}^{\infty} dx_c \rho(x_c) \int_{-G/2}^{G/2} dx_0 \int_{-G/2}^{G/2} dx (x - x_0)^2 \mathcal{P}_{x_c, x_0}(x, 0) \mathcal{P}_{x_c, x_0}(x, t)}{\int_{-\infty}^{\infty} dx_c \rho(x_c) \int_{-G/2}^{G/2} dx_0 \int_{-G/2}^{G/2} dx \mathcal{P}_{x_c, x_0}(x, 0) \mathcal{P}_{x_c, x_0}(x, t)}. \quad (5)$$

Short-time measurements of $\overline{\Delta x^2(t)}$ can be used (Giuggioli et al., 2004; Abramson et al., 2004) to obtain the diffusion constant D . In the present paper we are interested only in the home ranges, consequently in the infinite time limit of Eq. (5) which requires only the steady state solution.

Analytic solutions of the Fokker-Planck equation for all times are known only for very few cases of $U(x)$. However, steady state solutions are known for any potential explicitly in terms of an integral (Risken, 1989; Kuš and Kenkre, 1992; Parris et al., 2001)

$$\mathcal{P}_{x_c, x_0}(x, t \rightarrow +\infty) = \frac{e^{-U(x-x_c)/D}}{\int_{-\infty}^{\infty} dx' e^{-U(x')/D}}. \quad (6)$$

Equation (5) for $t \rightarrow \infty$ can, thus, be written as

$$\overline{\Delta x_{ss}^2} = \frac{\int_{-\infty}^{\infty} dx_c \rho(x_c) \int_{-G/2}^{G/2} dx_0 \int_{-G/2}^{G/2} dx (x - x_0)^2 e^{-\frac{U(x_0-x_c)+U(x-x_c)}{D}}}{\int_{-\infty}^{\infty} dx_c \rho(x_c) \int_{-G/2}^{G/2} dx_0 \int_{-G/2}^{G/2} dx e^{-\frac{U(x_0-x_c)+U(x-x_c)}{D}}}, \quad (7)$$

and further reexpressed in terms of quantities related to moments of the steady state probability density, equivalently of $\exp[-U(x)/D]$:

$$\overline{\Delta x_{ss}^2} = 2 \left\{ \int_{-\infty}^{\infty} dx_c \rho(x_c) \left[\left(\int_{-G/2-x_c}^{G/2-x_c} dx e^{-\frac{U(x)}{D}} \right) \left(\int_{-G/2-x_c}^{G/2-x_c} dx x^2 e^{-\frac{U(x)}{D}} \right) - \left(\int_{-G/2-x_c}^{G/2-x_c} dx x e^{-\frac{U(x)}{D}} \right)^2 \right] \right\} \left\{ \int_{-\infty}^{\infty} dx_c \rho(x_c) \left[\left(\int_{-G/2-x_c}^{G/2-x_c} dx e^{-\frac{U(x)}{D}} \right)^2 \right] \right\}^{-1} \quad (8)$$

The expression (7) can be reduced further if the burrow distribution $\rho(x_c)$ is uniform in space. We obtain

$$\overline{\Delta x_{ss}^2} = \frac{G \int_{-G}^G dy y^2 g(y) - \left(\int_0^G dy y^3 g(y) - \int_{-G}^0 dy y^3 g(y) \right)}{G \int_{-G}^G dy g(y) - \left(\int_0^G dy y g(y) - \int_{-G}^0 dy y g(y) \right)}, \quad (9)$$

where $g(y)$ is the convolution of $\exp[-U(x)/D]$ with itself:

$$g(y) = \int_{-\infty}^{\infty} dx_c e^{-\frac{U[x_c]+U[x_c-y]}{D}}. \quad (10)$$

If the potential $U(x)$ remains finite for all finite values of x , $g(y) = g(-y)$, and it is possible to write a simpler form of (9):

$$\overline{\Delta x_{ss}^2} = \frac{\int_0^G dy (G-y) y^2 g(y)}{\int_0^G dy (G-y) g(y)}. \quad (11)$$

Clearly, the trapping array of width G can be interpreted as a probe into the system whose characteristic width is L . The mean square displacement depends on the relative magnitude of L and G of the probe. In the limit of an infinitely large probe, $(\overline{\Delta x_{ss}^2})^{1/2}$ measures simply the characteristic length of the system. It is thus natural to define the home range length L for *arbitrary potentials* as the square root of the limit $G \rightarrow \infty$ of Eq. (9),

$$L = \sqrt{\frac{\int_{-\infty}^{+\infty} dy y^2 g(y)}{\int_{-\infty}^{+\infty} dy g(y)}}, \quad (12)$$

when such a limit exists. If the probe is very small compared to the home range width, the trapping array will measure a quantity associated with the width of the grid. In fact $g(y)$ becomes a constant in the limit $L \rightarrow \infty$ and Eq. (11) gives $G^2/6$ for the mean square displacement ^{*}.

In a recent article, one of the present authors (Kenkre, 2005) has given an alternate formulation in terms of the Fourier transform of the steady state probability distribution (6). It has been shown there that the mean square displacement is given simply in terms of Fourier-space integrals of the product

^{*} While the definition (12) of the home range L is the most natural, alternate definitions are possible as used, e.g., in (Abramson et al., 2004).

of the square of the sinc function (which carries information about the probe) with respectively the square, and the derivative of the square, of the transform of the steady state probabilities (which carry information about the home ranges). Alternative expressions equivalent to Eq. (9) and (12), respectively, are given in (Kenkre, 2005) as

$$\overline{\Delta x_{ss}^2} = - \frac{\int_{-\infty}^{\infty} dk \frac{\partial^2 \widehat{P}^2(k)}{\partial k^2} \frac{[1 - \cos(Gk)]}{k^2}}{\int_{-\infty}^{\infty} dk \widehat{P}^2(k) \frac{[1 - \cos(Gk)]}{k^2}} \quad (13)$$

and

$$L^2 = -2 \left. \frac{\frac{\partial^2 \widehat{P}(k)}{\partial k^2}}{\widehat{P}(k)} \right|_{k=0} = 2 \frac{\int_0^{+\infty} dy y^2 e^{-\frac{U(y)}{D}}}{\int_0^{+\infty} dy e^{-\frac{U(y)}{D}}}, \quad (14)$$

where $\widehat{P}(k)$ is the Fourier transform of $\exp[-U(x)/D]$.

Clearly, a dimensionless quantity of crucial importance to the analysis is the ratio ζ of the home range to the observational probe length G :

$$\zeta = L/G. \quad (15)$$

In the next section we study the functional dependence of the saturation curve on this quantity ζ with attention to the effects of the details of the confining potential, assuming that $\rho(x_c)$ is a constant.

3 Dependence on the details of the confining potential

The precise shape of the confining potential $U(x)$ obviously depends on the detail of animal movement, such as habitat and distance between neighbours. Since this detail is largely unavailable, it is important to determine the sensitivity of the deduced value of the home range size L to the choice of $U(x)$. It is clear that, when plotted as a function of ζ (see Eq. (15)), the mean square displacement $\overline{\Delta x_{ss}^2}$ for each potential starts out as L^2 when $\zeta \rightarrow 0$ and saturates to $G^2/6$ when $\zeta \rightarrow \infty$.

Extensive studies we have carried out with different potentials have made it clear that the curvature at the bottom and the steepness with which $U(x)$ becomes infinite both play a role in shaping the saturation curve of $\overline{\Delta x_{ss}^2}$. More precisely, the rise of $\overline{\Delta x_{ss}^2}$ is controlled by the steepness of the potential when $x/L \gg 1$: the steeper the rise to infinity of the potential, the smaller the value of ζ for which the saturation curve grows faster than the L^2 dependence at $L = 0$. In addition, the curvature of $U(x)$ for $x/L \ll 1$ determines the way $\overline{\Delta x_{ss}^2}$ approaches the value $G^2/6$: the larger the curvature, the slower it approaches the asymptote $G^2/6$. In Fig. 1 we show this dependence by comparing four

characteristic potentials: a box potential, a harmonic potential and two types of logarithmic potentials.

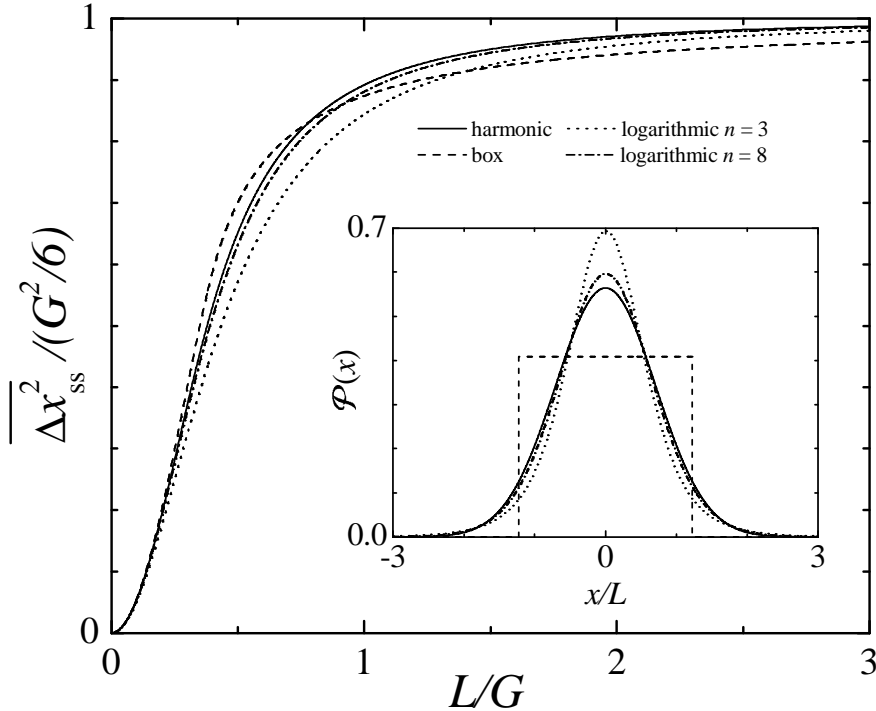


Fig. 1. Mean square displacement at saturation for four different potentials: a box potential (dashed line), a harmonic potential (solid line), and two logarithmic potentials (see text for definition) one with $n = 3$ (dotted line) and the other with $n = 8$ (dash-dotted line). The inset shows the corresponding stationary distributions $\mathcal{P}(x)$ as obtained from Eq. (6) by putting $x_c = 0$.

3.1 Box and harmonic potentials

The box potential has the steepest rise among the four curves in Fig. 1, since it diverges at a finite distance. Observe also that it is the slowest to reach $G^2/6$, being the one with the smallest curvature (zero) close to the origin. Such a potential has been considered in our previous work (Giuggioli et al., 2004; Abramson et al., 2004) for extracting home range sizes from mark-recapture data for two different rodent populations. In those investigations the saturation curve was numerically simulated. However, it is possible to calculate analytically all the integrals in Eq. (8) by selecting judiciously the limit of integration for the variable x_c as function of the relative dimension of the box

width and the probe width. The resulting expression in terms of ζ is given by

$$\frac{\overline{\Delta x_{ss}^2}}{G^2/6} = \begin{cases} \frac{18\zeta^2}{5} \frac{(5-3\sqrt{6}\zeta)}{(3-\sqrt{6}\zeta)}, & \text{for } \zeta < \sqrt{6}, \\ \frac{3}{5} \frac{(3-5\sqrt{6}\zeta)}{(1-3\sqrt{6}\zeta)}, & \text{for } \zeta > \sqrt{6}. \end{cases} \quad (16)$$

The limiting behaviour is that $\overline{\Delta x_{ss}^2} \simeq L^2$ for small ζ and $\overline{\Delta x_{ss}^2} \simeq G^2/6 - 4/(15\sqrt{6}\zeta)$ for large ζ .

The harmonic potential has been used in one of our previous studies (Abramson et al., 2004) for extracting the home range size for the deer mouse, *Peromyscus maniculatus*, in New Mexico. The shape of the potential is given by $U(x) = D(x/L)^2$. Since the domain where $U(x)$ is not zero extends over the entire real axis, it is convenient to calculate the convolution (10) which gives $g(y) = L\sqrt{\pi/2} \exp[-y^2/(2L^2)]$. Integrating Eq. (11) gives the mean square displacement at saturation as

$$\frac{\overline{\Delta x_{ss}^2}}{G^2/6} = 6\zeta^2 \left\{ 1 + \frac{\sinh[(1/2\zeta)^2]}{\sinh[(1/2\zeta)^2] - \frac{1}{2\zeta}\sqrt{\frac{\pi}{2}}e^{(1/2\zeta)^2} \operatorname{erf}\left(\frac{1}{\sqrt{2}\zeta}\right)} \right\}, \quad (17)$$

with $\overline{\Delta x_{ss}^2} \simeq L^2$ when $\zeta \ll 1$ and $\overline{\Delta x_{ss}^2} \simeq G^2/6 [1 - (7/120\zeta^2)]$ when $\zeta \gg 1$. The intersection in Fig. 1 between the harmonic potential curve (solid) and the box potential curve (dashed) becomes evident here given that the former approaches $G^2/6$ linearly while the latter approaches it quadratically as $\zeta \rightarrow \infty$.

3.2 Logarithmic potentials

As an example of $U(x)$, whose corresponding steady state distribution given by (6) decays to zero slower (algebraically) than in the box or the harmonic case, we consider a family of potentials of the form

$$U(x) = D \ln \left\{ 1 + \frac{x^2}{(\kappa_n L)^2} \right\}^n, \quad (18)$$

with $\kappa_n = \sqrt{n - 3/2}$ and $n \geq 2$. These potentials have a quadratic dependence when $x/L \ll 1$ and a logarithmic dependence for $x/L \gg 1$ such that $\mathcal{P}(x) \simeq x^{-2n}$ as $|x| \rightarrow \infty$. It is straightforward to check that the expression (18) is consistent with the definition (12) of the home range L for any value of n . In the limit of $n \rightarrow +\infty$ (18) reduces to the harmonic case. We have studied, in particular, the cases from $n = 2$ to $n = 8$ and have obtained analytical expressions for the mean square displacement. We do not display them here because they do not add to the understanding. In Fig. 1 we show the cases $n = 3$ and $n = 8$. Already for $n = 8$ the saturation curve for the logarithmic

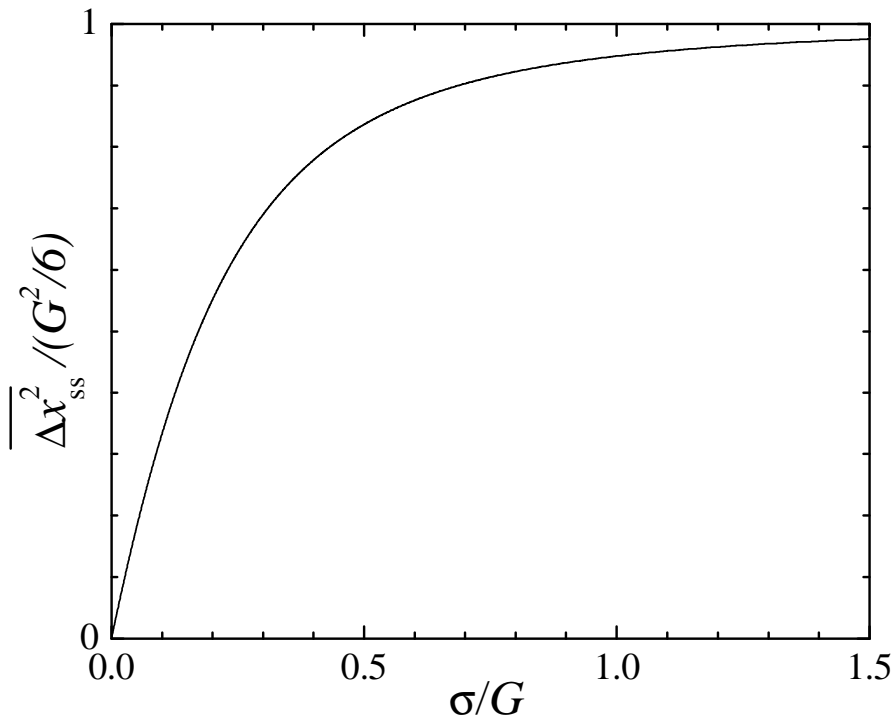


Fig. 2. Mean square displacement at saturation for the potential $U(x) = D \ln(1 + (x/\sigma)^2)$. Compared to the potentials depicted in Fig. 1, here $U(x)$ grows to infinity qualitatively slower. The corresponding distribution $\mathcal{P}(x)$ does not possess a finite second moment. The long-tailed distribution changes drastically the behaviour of $\overline{\Delta x_{ss}^2}$ when very large grid sizes are used. The growth of the saturation curve for small σ/G is linear and not quadratic.

and the harmonic cases are very close to each other. The inset of Fig. 1 shows the origin of such similarities by comparing the corresponding steady state probability distributions $\mathcal{P}(x)$.

As mentioned above, the $\mathcal{P}(x)$ associated with the logarithmic potentials possesses long tails. Probability distributions with long tails can be appropriate when the motion of the animal cannot be represented by a simple random walk. More complex types of walk may occur if the walker awaits for very long times between jumps, or if the jumps are of very large distance. Long-tailed $\mathcal{P}(x)$ are characterized by the feature that certain moments of the distribution become infinite. If all the moments beyond the first are infinite, Eq. (12) is no longer applicable for defining the home range width. A qualitatively different behaviour is expected for large values of G . To illustrate this situation, we

consider the potential

$$U(x) = D \ln\left(1 + \frac{x^2}{\sigma^2}\right) \quad (19)$$

whose corresponding $\mathcal{P}(x)$ is the Cauchy distribution (Lemons, 2002) $\mathcal{P}(x) = (1 + (x/\sigma)^2)^{-1}/\pi$. Also for this case the mean square displacement can be obtained analytically and it is given by

$$\frac{\overline{\Delta x_{ss}^2}}{G^2/6} = 6 \left[\frac{\xi}{\tan^{-1}\left(\frac{1}{2\xi}\right) - \xi \ln\left(1 + \frac{1}{(2\xi)^2}\right)} - 4\xi^2 \right], \quad (20)$$

where $\xi = \sigma/G$. As $\xi \rightarrow 0$, $\overline{\Delta x_{ss}^2}/(G^2/6) \simeq (12/\pi)\sigma/G$ in Eq. (20). A linear growth of the saturation curve emerges, as depicted in Fig. 2. Notice that L , as defined by Eq. (12), does not exist for this potential. The home range is therefore defined as the characteristic length σ , the ratio ξ being the counterpart of ζ of (15). This different qualitative behaviour with respect to the previously analyzed cases could be exploited for determining the characteristics of the animal walks by making various measurements with large grid size. A sufficient number of these measurements would allow one to discern if the saturation curve is growing quadratically (as in the examples of Fig. 1) or linearly (as in Fig. 2).

The examples of this section illustrate that the choice of $U(x)$ in any application of the present theory should be assessed in each case, based, for example, on a priori knowledge of the specific animal behavior. The different potentials shown here give an overview of the possible qualitative behaviours of the mean square displacement at saturation.

4 Inhomogeneous distribution of home ranges: the case of a periodic arrangement

The results obtained in Sec. 2, from Eq. (9) onward, and the examples developed in Sec. 3, assume a continuous and homogeneous distribution of burrow location x_c . A more realistic situation invokes the home ranges arranged in a non-continuous manner, the centers of adjacent ranges (the burrow locations) separated by some characteristic distance a . In this section we show an example of how this feature may be incorporated in our analysis and how, in principle, a can be deduced from mark-recapture measurements.

Let us suppose for simplicity that the home ranges are distributed in a periodic array, with a being the distance between nearest neighbors. The mean square displacement, measured within a window of linear size G , is now a function of a and L , besides depending parametrically on G . As in Section 2, G can be used to rescale the two coordinates a and L . The function

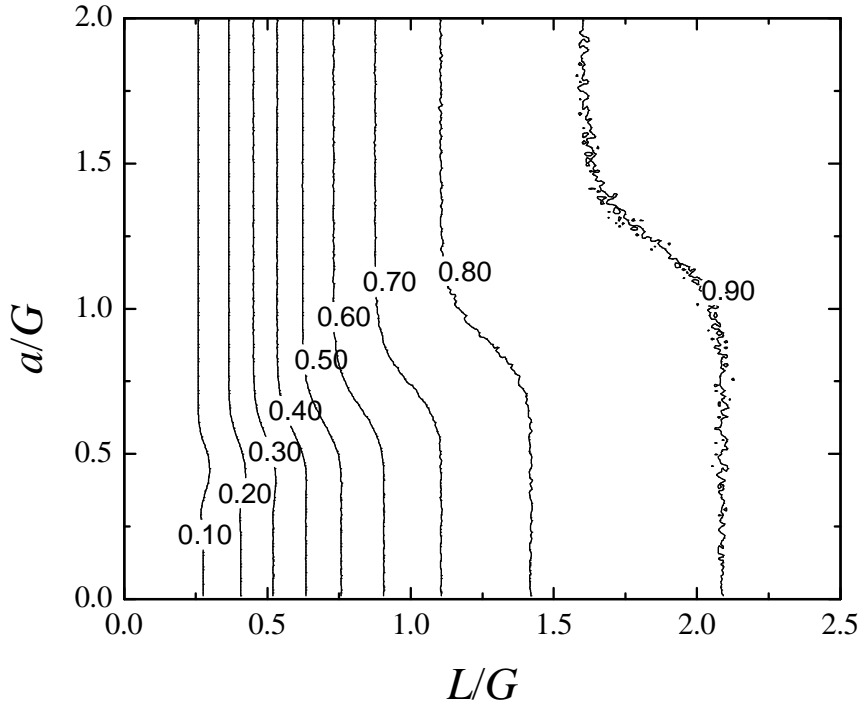


Fig. 3. Contour plot of the normalized mean square displacement, $\overline{\Delta x_{ss}^2}/(G^2/6)$, as a function of the normalized home range size, L/G and the normalized inter-home distance, a/G . The lines are the result of simulations of the harmonic model (Gaussian occupation of space). The fluctuations in the lines are an artifact of the construction of the contours from discrete simulations.

$\overline{\Delta x_{ss}^2}/(G^2/6) = f(L/G, a/G)$ is universal and does not depend on the size of the observation window. We show a contour plot of this function in Fig. 3, as calculated by numerical simulation of the harmonic model (Gaussian probability distributions). At $a = 0$, the shape of the surface coincides with the curve calculated in Eq. (17). The contours of equal mean square displacement are nearly vertical lines in this plot, indicating that the dependence on the inter-home distance a is very weak (in particular for small values of the normalized mean square displacement), except for a region well defined in a , where the contours shift from one value of L to another. This feature will certainly be of relevance if an experiment is designed in order to measure both a and L , since the uncertainty on a will tend to be large.

In general, given that the function $\overline{\Delta x_{ss}^2}$ is nonlinear in both its variables a/G and L/G , two or more measurements are necessary to determine the home range size and the inter-home distance. In Fig. 4 we show a hypothetical situation in which three measurements are supposed to be taken on the same

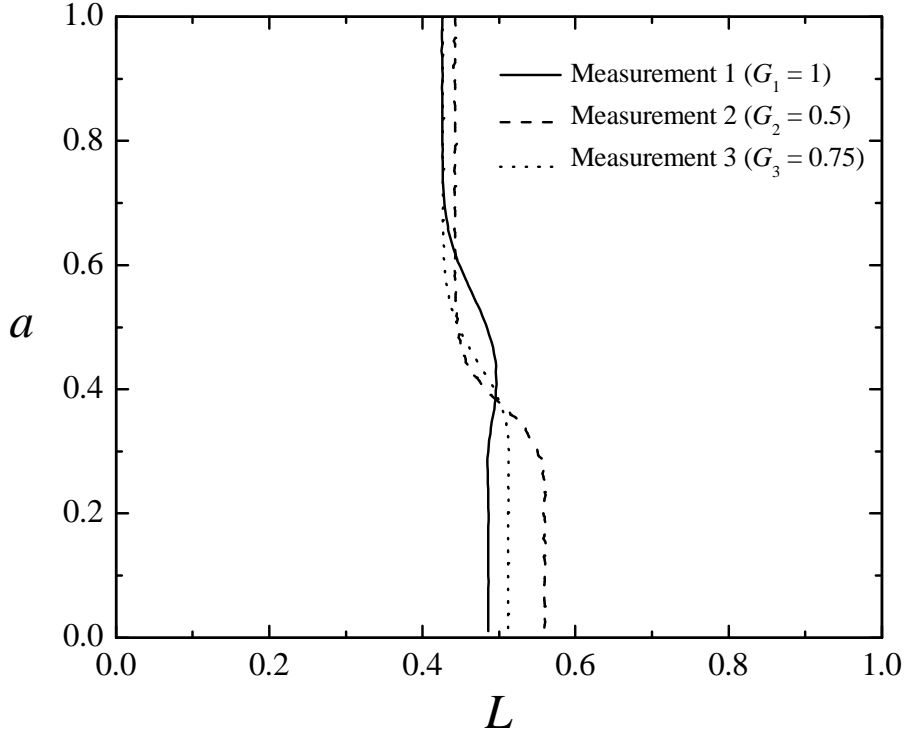


Fig. 4. Graphical explanation of the procedure to determine home range overlap via a hypothetical measurement. Both L and a can be determined by taking three measurements of the same population, using three windows, of sizes G_1 , G_2 and G_3 . The measured mean square displacements are supposed to be $\overline{\Delta x_1^2} = 0.045$, $\overline{\Delta x_2^2} = 0.029$, and $\overline{\Delta x_3^2} = 0.041$. The corresponding contours intersect at $L = 0.5$, $a = 0.375$, providing these values as a result. Both a and L are displayed in units of G (arbitrary linear units).

population, using three windows sizes, $G_1 = 1$, $G_2 = G_1/2$ and $G_3 = 3G_1/4$. The results of the measurement are curves of constant $\overline{\Delta x_{ss}^2}$ in the plane (L, a) . With three measurements, $\overline{\Delta x_1^2}$, $\overline{\Delta x_2^2}$ and $\overline{\Delta x_3^2}$, three curves are obtained, and the model predicts:

$$\begin{aligned}
 \overline{\Delta x_1^2}/(G_1^2/6) &= f(L/G_1, a/G_1), \\
 \overline{\Delta x_2^2}/(G_2^2/6) &= f(L/G_2, a/G_2), \\
 \overline{\Delta x_3^2}/(G_3^2/6) &= f(L/G_3, a/G_3).
 \end{aligned}
 \tag{21}$$

This is a system of three (nonlinear) equations with two unknowns, L and a , and its solution can be found as the intersection of three curves. These curves are shown in Fig. 4, displaying an intersection very near $L = 0.5$, $a = 0.375$ (within the accuracy of the fluctuations of the contours). The curves were obtained from the normalized function, shown in Fig. 3, using the appropriate contours. As mentioned above, the weak dependence on a may hinder its

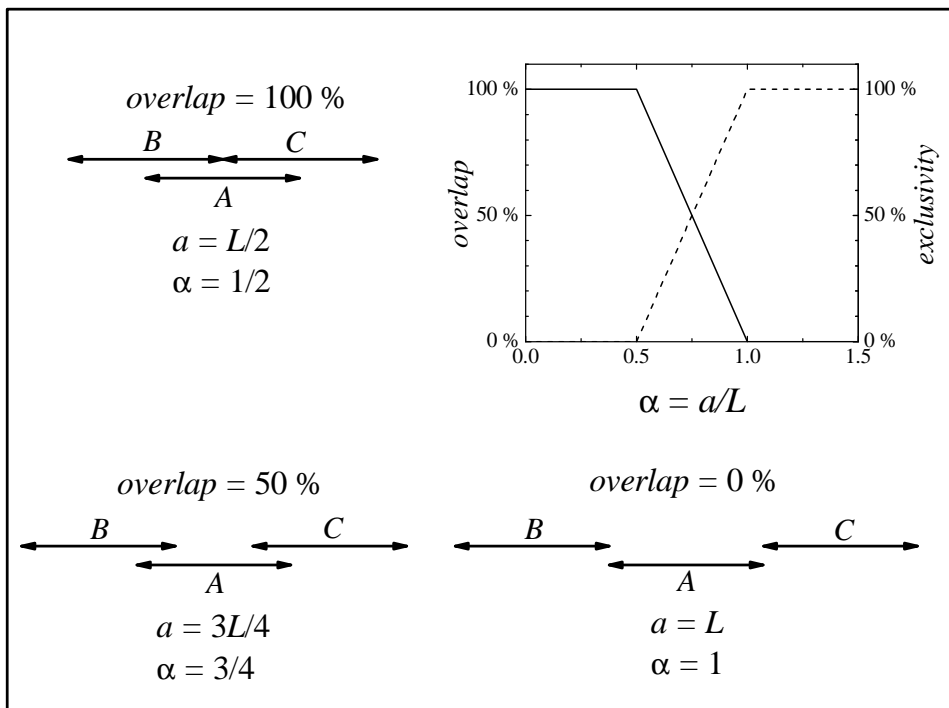


Fig. 5. Illustration of home range overlap situations, and the variables characterizing them. The schematic diagram shows three cases: 100%, 50%, and 0% overlap, with arrows representing the extent of the home range of three neighbouring animals, A, B and C. The plot shows the relation between the overlap, the exclusivity of space use, and the normalized inter-home distance $\alpha = a/L$.

determination by the present method. It is clear that the choice of the appropriate values of the window sizes is critical to obtain the best results. This must be done specifically for each situation, with the help of an informed guess of the range where both a and L lie. Regardless of this practical difficulty, the procedure we describe provides a method for an immediate measurement of an important quantity that is hard to obtain by other means. Additionally, if the population is not well characterized by a typical inter-home distance, as we suppose here (for example, if the inter-home distance is bimodal due to gender differences or other polymorphism), the model can be immediately modified to incorporate those features.

Moreover, the inter-home distance is closely related to the overlap of home ranges (or to the exclusivity of space use). See Fig. 5 for an illustration of three typical situations. The home ranges of three neighbouring animals, A, B, and C, are displayed as arrows, schematically representing the extent of the area occupied by 95% of the norm of $\mathcal{P}(x)$, as usually defined (Worton, 1987). When $a = L/2$, the first neighbours, B and C, of A have their home ranges situated at the border of A's home range. Then, A does not have exclusive

use of any part of its own home range (overlap equal 100%). On the other extreme, when $a = L$, the home ranges of B and C are completely outside A 's. In consequence, the exclusivity of A is 100% (home range overlap 0%). This value of exclusivity, certainly, is maintained for any value of $a > L$. An intermediate situation, in which the exclusivity of animal A is equal to 50% (as well as its overlap with the neighbours) is also shown.

The exclusivity of space use has recently been found to obey an allometric scaling relation with the animal mass by Jetz et al. (2004). The present theory provides a method to determine both the home range size and the home range overlap, and thus to verify the scaling of these and related magnitudes (West et al., 1997; Banavar et al., 1999).

5 Comparison with convex polygon calculations

Home range sizes have been often deduced from the measurement of the so-called minimum convex polygon of an animal position. Although this procedure suffers from a number of drawbacks (Worton, 1987), it is used rather widely. Among its drawbacks it is easy to recognize at least a logical and a methodological one. The surveyed perimeter provides no information about the use of space inside it, effectively encompassing areas that may be inaccessible to the animal, or potentially huge areas of very low frequency of utilization. The methodological one is the fact that the measured area converges very slowly to the actual home range, and as such the observation of a few tens of positions provides a very bad estimation. Both kinds of flaws have been recognized in the literature before (see Worton (1987) and references therein), and suggestions have been made to compensate for them. These proposals, such as discarding some fraction of the extreme positions from a set of observations to compensate for the first, or to join the perimetral points in a fashion different from the minimum convex polygon, are surely arbitrary. Furthermore, methodologically, they are obviously subject to uncontrollable errors.

In the following we illustrate how the calculation of the mean square displacement we have given in the present paper provides a rapidly converging measurement of the home range size. This is an additional advantage when displacements of animals belonging to a population are more readily accessible than repeated measurements of the position of individual animals. For the sake of the illustration, we will consider that the probability of space use of an animal is a bivariate Gaussian distribution of variance σ :

$$\mathcal{P}(x, y) = \frac{1}{2\pi\sigma^2} e^{-\frac{x^2+y^2}{2\sigma^2}}. \quad (22)$$

We consider this symmetric distribution for simplicity, but the discussion applies equally to a distribution with anisotropic σ . Moreover, the conclusions are equivalent for more general distributions, including those with a finite cut-off.

If we define the home range of the animal whose space use distribution is described by (22) as the area A that contains the 95% of \mathcal{P} (Worton, 1987), a simple integration gives

$$A = \pi R^2 = 2\pi\sigma^2(-\ln 0.05) \approx 18.8\sigma^2. \quad (23)$$

This the quantity that we intend to measure by both methods. In Fig. 6 we show the area of the minimum convex polygon defined by a set of N points

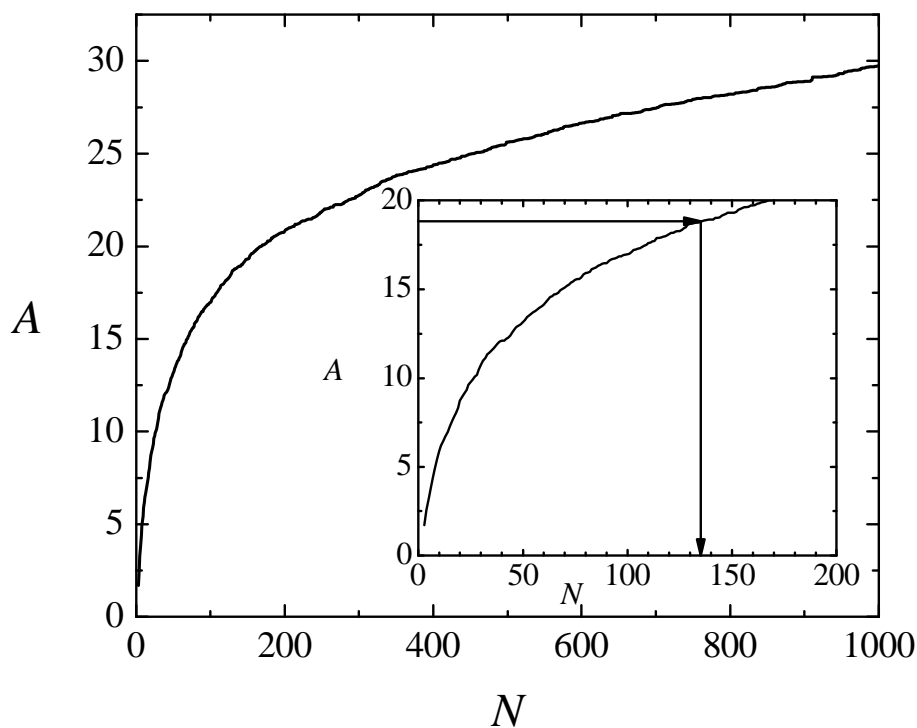


Fig. 6. Area A enclosed by the minimum convex polygon corresponding to a set of random points with Gaussian distribution in the plane, as a function of N , the number of points of the set. The line shows the average of 50 independent realizations. The inset shows a detail of the same function, with arrows showing the necessary number of points to obtain a good measurement of the home range, defined as the 95% of the space occupation which, for $\sigma = 1$, and $A \approx 18.8$, is $N = 135$ points. The variance σ has arbitrary units of length, and A those of length squared.

drawn at random with a bivariate Gaussian distribution of $\sigma = 1$. Observe, firstly, that the area grows unboundedly as the number of observations grows, since \mathcal{P} is unbounded. More relevant from the practical point of view is the fact that the growth is very slowly, and that the area A (obtained with 95% rule and marked in Fig. 6 with an arrow) is achieved after the observation contains, on average, 135 points (see the inset of Fig. 6).

Now consider that one wants to determine A by measuring *displacements*, instead of positions. The relevant quantity to be estimated is the variance σ , immediately derived from the home range size L , accessible through our present theory explained in Sec. 2. Expression (23) gives then the home range area. Figure 7 shows that the measurement of the variance, σ_N , for a finite set of N observations, converges very rapidly to the actual value (which is 1 in this case), when the number of observations is increased. Indeed, with just 10 observations of the displacement the variance can be estimated with an accuracy greater than 95%. Ten displacements correspond to just 11 positions of a single animal, if taken at intervals long enough that they are uncorrelated,

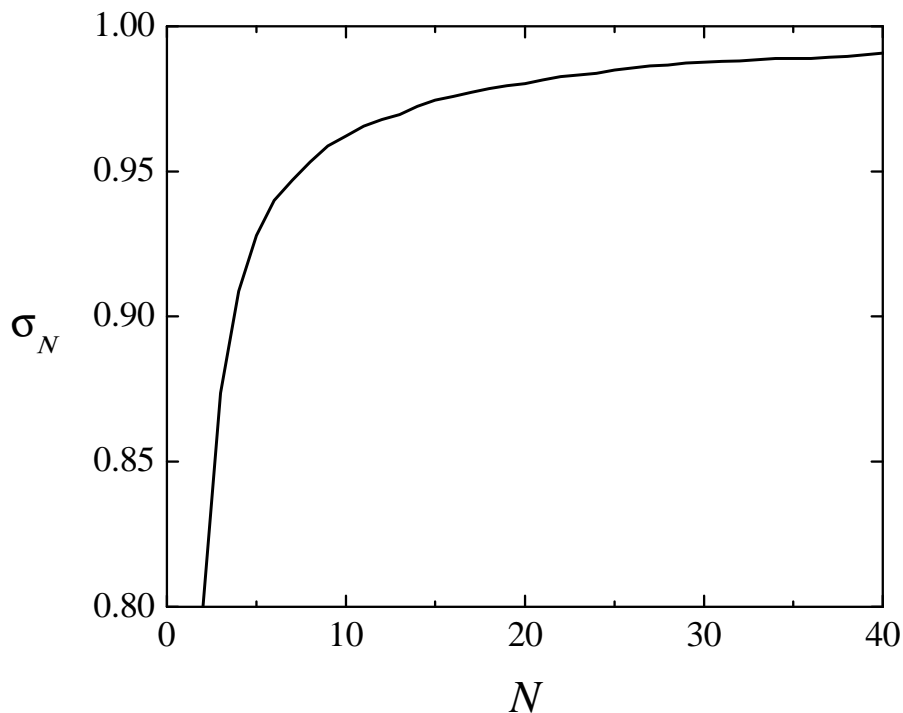


Fig. 7. Measurement of the variance of a bivariate Gaussian distribution ($\sigma = 1$), as a function of the number of displacements used for the estimate. The curve shows an average based on 104 realizations.

or 10 displacements of different animals for which an average distribution would be found.

In summary, the mean square displacement provides a faster convergence to the area of the home range than the construction of the convex polygon. In addition, the estimation of the distribution \mathcal{P} (unimodal in this case, but easily generalizable) by that method provides information about the use of the home range, which is inaccessible to the convex polygon procedure.

6 Conclusions

The determination of home range dimensions and spatial overlap of two neighbouring home ranges from field observation is a subject of great interest for the understanding of animal motion. We have provided here a general theory to extract such demographic parameters on the basis of the measurement of displacements of individual animals in a population.

The most common techniques for gathering information of home range size employ trapping of animal and radiotelemetry observations. Our theory in the present paper has been constructed with the specific goal of interpreting data obtained from the former type of observation, i.e., mark-recapture experiments, in which the sampling area is finite.

The motion of an animal inside its own home range has been modeled by a Fokker-Planck equation (1), i.e. by diffusion in a confining potential $U(x)$. While the equations considered are, for simplicity, 1-dimensional, extension to higher dimensions is straightforward and unnecessary for practical purposes.

Even though the precise determination of the home range size L depends on the choice of the potential $U(x)$, the general sigmoid shape of the saturation curve in our theory indicates that the difference in the results is not substantial if the window size is chosen such that $L < G$. Eventually, the choice of the right potential is to be determined for each given case, on the basis of biological information of the animal population under study. We have shown that, for those situations in which the second moment of the distribution $\mathcal{P}(x) = \exp(-U(x)/D)$ is not finite, the saturation curve for large G grows linearly with L rather than quadratically as in more conventional potentials (box or harmonic). Such cases may arise when the animal motion is not simple but involve a more complicated random walk such as a Levi walk or flight. This means that our theory of mark-recapture observation may be used, in principle, to determine whether the animal population is performing a Gaussian random walk or a more complicated walk. By measuring the mean square displacement at saturation with different values of the probe length G

(sufficiently larger than L) it might be possible to determine if the saturation curve grows quadratically or linearly.

The obtained parameters that characterize the average use of space, when obtained via mark-recapture observations and their interpretation with our present theory, converge rapidly to the expected values. We have shown in Sec. 5 that this is not the case in the application of the traditional minimum convex polygon method. We thus suggest that displacement measurements of an animal population should be considered as the most appropriate way for determining home range dimensions if radiotelemetry methods are not available.

The other important demographic parameter that can be extracted from mark-recapture measurements is the inter-home characteristic distance of the animals, called a in the present paper. Such a length is simply related to the mean overlap (or the mean exclusivity of space usage). We have outlined a procedure to extract this parameter quantitatively from mark-recapture observations and provided a general way to verify directly from mark-recapture experiments the scaling of home range overlap as function of body mass.

Acknowledgements

It is a pleasure to thank Marcelo Kuperman and Ignacio Peixoto for fruitful discussions. This work was supported in part by the NSF under grant no. INT-0336343, by NSF/NIH Ecology of Infectious Diseases under grant no. EF-0326757 and by DARPA under grant no. DARPA-N00014-03-1-0900. G. Abramson acknowledges partial funding by CONICET (PEI 6482), and by Fundación Antorchas.

References

- Abramson, G. and Kenkre, V.M., 2002. Spatio-temporal patterns in the Hantavirus infection. *Phys. Rev. E* 66, 011912-1-5.
- Abramson, G., Kenkre, V.M., Yates, T.L. and Parmenter, R.R., 2003. Traveling waves of infection in the Hantavirus epidemics. *Bull. Math. Biol.* 65, 519-534.
- Abramson, G., Giuggioli, L., Kenkre, V.M., Dragoo, J.W., Parmenter, R.R., Parmenter, C.A. and Yates, T.L., 2004. Diffusion and Home Range Parameters for Rodents II. *Peromyscus maniculatus* in New Mexico, submitted to *Ecol. Complexity*.
- Anderson, D.J., 1982. The home range, a new nonparametric estimation technique. *Ecology* 63(1), 103-112.

- Banavar, J.R., Maritan, A. and Rinaldo, A., 1999. Size and form in efficient transportation networks. *Nature* 399, 130-132.
- Bergstrom, B.J., 1988. Home ranges of three species of chipmunks (*Tamias*) as assessed by radiotelemetry and trapping. *J. Mammal.* 69, 190-193.
- Burt, W.H., 1943. Territoriality and home range concepts as applied to mammals. *J. Mammal.* 24, 346-352.
- Buskirk, S., 2004. Keeping an eye on the neighbors. *Science* 306, 238-239.
- Ford, R.G. and Krumme, D.W., 1979. The analysis of space use patterns. *J. Theor. Biol.* 76, 125-155.
- Giuggioli, L., Abramson, G., Kenkre, V.M., Suzán, G., Marcé, E. and Yates, T.L., 2004. Diffusion and Home Range Parameters from Rodent Population Measurements in Panama. *Bull. Math. Biol.* (accepted for publication).
- Jennrich, R.I. and Turner, F.B., 1969. Measurement of non-circular home range. *J. Theor. Biol.* 22, 227-237.
- Jetz, W., Carbone, C., Fulford, J. and Brown, J.H., 2004. The scaling of animal space use. *Science* 306, 266-268.
- Kenkre, V.M., 2003. Memory formalism, nonlinear techniques, and kinetic equation approaches, in: Kenkre, V. M., Lindenberg, K. (Eds.), *Modern Challenges in Statistical Mechanics: Patterns, Noise, and the Interplay of Nonlinearity and Complexity*, AIP Proc. vol. 658, Melville, NY, pp. 63-102.
- Kenkre, V.M., 2004. Results from the variants of the Fisher equation in the study of epidemics and bacteria. *Physica A* 342, 242-248.
- Kenkre, V.M., Abramson, G., Giuggioli, L., Camelo Neto, G., 2004. Generalized Models for the Spread of Hantavirus. In preparation.
- Kenkre, V.M., 2005. Statistical Mechanical Considerations in the Theory of Epidemics. In preparation.
- Kuś, M. and Kenkre, V.M. 1992. Stochastic derivation of the switching function in the theory of microwave heating of ceramic materials. *Phys. Rev. B* 45, 9695-9704.
- Lemons, D.S., 2002. *An introduction to stochastic processes in physics*. Johns Hopkins University Press, Baltimore.
- Mares, M.A., Willig, M.R. and Bitar, N.A., 1980. Home range size in Eastern chipmunks, *Tamias striatus*, as a function of number of captures: statistical biases of inadequate sampling. *J. Mammal.* 61, 661-669.
- Murray, J.D., 1993. *Mathematical Biology*, 2nd edition. Springer-Verlag, New York.
- Okubo, A., 1980. *Diffusion and Ecological Problems: Modern Perspectives*, 2nd. edition. Springer-Verlag, Berlin.
- Parmenter, R.R. and MacMahon, J.A., 1983. Factors determining the abundance and distribution of rodents in a shrub-steppe ecosystem: the role of shrubs. *Oecologia* 59, 145-156.
- Parmenter, R.R., Yates, T.L., Anderson, D.R., Burnham, K.P., Dunnun, J.L, Franklin, A.B., Friggens, M.T., Lubow, B.C., Miller, M., Olson, G.S., Parmenter, C.A., Pollard, J., Rexstad, E., Shenk, T.M., Stanley T.R. and White, G.C., 2003. Small-mammal density estimation: a field comparison

- of grid-based vs. web-based density estimators. *Ecological monographs* 73, 1-26.
- Parris, P.E., Kuś, M. and Kenkre, V.M., 2001. Fokker-Planck analysis of the nonlinear field dependence of a carrier in band at arbitrary temperatures. *Phys. Lett. A* 289, 188-192.
- Risken, H., 1989. *The Fokker-Planck equation: methods of solution and applications*. Springer-Verlag, New York.
- West, G.B., Brown, J.H. and Enquist, B.J., 1997. A general model for the origin of allometric scaling laws in biology. *Science* 276, 122-126.
- Wolff, J.O., 1997. Population regulation in mammals: an evolutionary perspective. *J. Animal Ecol.* 66, 1-13.
- Worton, B.J., 1987. A review of models of home range for animal movement. *Ecol. Modelling* 38, 277-298.
- Yates, T. L., Mills, J. N., Parmenter, C. A., Ksiazek, T. G., Parmenter, R. R., Vande Castle, J. R., Calisher, C. H., Nichol, S. T., Abbott, K. D., Young, J. C., Morrison, M. L., Beaty, B. J., Dunnnum, J. L., Baker, R. J., Salazar-Bravo, J. and Peters, C. J., 2002. The ecology and evolutionary history of an emergent disease: Hantavirus Pulmonary Syndrome. *Bioscience* 52, 989-998.